ACS OMEGA

http://pubs.acs.org/journal/acsodf

Article

Study on the Flow State of Circulating Cooling Water for the Industrial Heat Exchange Tube in the Electromagnetic Anti-Fouling Process

Lei Yan, Xiao Qi, Xing Han, Jianguo Wang, and Fang He*

Cite This: *ACS Omega* 2021, 6, 28515−28527

Read Online

ACCESS | Metrics & More | Article Recommendations

ABSTRACT: Comparing with the traditional chemical and physical method, the electromagnetic water treatment technology draws more attention of researchers for its advantages of easy application, small investment, low cost, and being pollution free in recent years. However, due to the less study of the formation process and adhesion of fouling on the surface of heat exchange equipment, the electromagnetic anti-fouling performance cannot be well evaluated. This paper studies the numerical simulation of the flow states of circulating cooling water in heat exchange tubes with a straight shape and U-shaped ones and analyzes the experimental data of fouling resistance on heat transfer surface under the action of 0.5, 0.75, 1, and 1.5 kHz electromagnetic fields. The variations in the velocity field and pressure field at various points in heat exchange tubes declare that the velocity of the circulating cooling water is smaller in the outlet of the pipeline. The change of the circulating cooling water flow state with the pipeline shape causes a certain impact on fluid velocity, and the pressure value at the outlet is larger. It is obtained that the flow velocity in the area with high surface pressure of circulating cooling water is relatively small. The experimental results indicate that the fouling resistance on the surface of the magnetic heat exchange tube is smaller than that of the nonmagnetic one. The anti-fouling efficiency in 0.5, 0.75, 1, and 1.5 kHz magnetic and contrast experiments are 46.8, 84.8, 91.2, and 63.6%, respectively. Better anti-fouling performances are obtained under the action of about 1 kHz electromagnetic frequency. The induction period of fouling on the heat exchange surface is lengthened under electromagnetic fields. All these studies are of significant importance to further understand the formation process and adhesion of fouling on the surface of heat exchange equipment, as well as to better evaluate the electromagnetic anti-fouling performance.

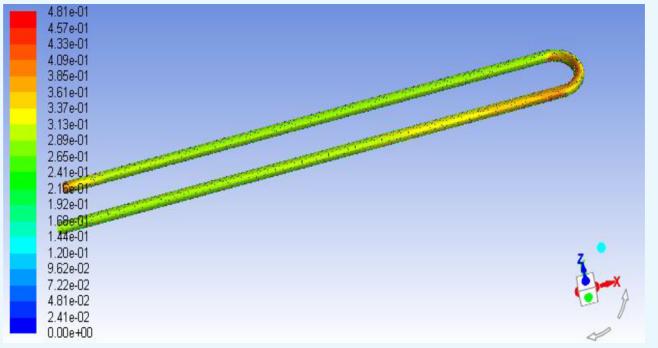

1. INTRODUCTION

In industrial production, the concentration of circulating cooling water has become a major issue related to the fouling phenomenon of on-site heat-exchange equipment, which brings about the fouling problem.[1] Chemical water treatment technology based on a water treatment agent is mature and widely used to suppress scaling, biological fouling, and corrosive fouling, which plays a leading role in the research of water treatment. However, chemical fouling removal and inhibition will cause serious environmental pollution problems and is high-cost with less effectiveness. Variable-frequency electromagnetic water treatment technology is employed due to its advantages of easy application, small investment, low cost, and being pollution free.[2]

Electromagnetic fields have significant influence on the fouling formation process of industrial heat-transfer equipment.[3] The effect of electromagnetic anti-fouling technology on fouling mitigation in a heat exchanger has gained wide attention.[4] There are sufficient works on chemical and physical methods for fouling removal and inhibition, though the mechanism and effectiveness of electromagnetic water treatment technology have not been fully studied.[5] This paper conducts numerical simulation research on the flow states of circulating cooling water, as well as experimental analysis for the characteristics of fouling resistance in the electromagnetic anti-fouling process, to further draw conclusions regarding the pace for fouling formation and adhesion of fouling on the surface of heat exchange equipment. Flow states include fluid property parameters (dynamics characteristics of fluid flow, water quality parameters, etc.)

Received: April 27, 2021
Accepted: October 12, 2021
Published: October 20, 2021

https://doi.org/10.1021/acsomega.1c02193
ACS Omega 2021, 6, 28515−28527

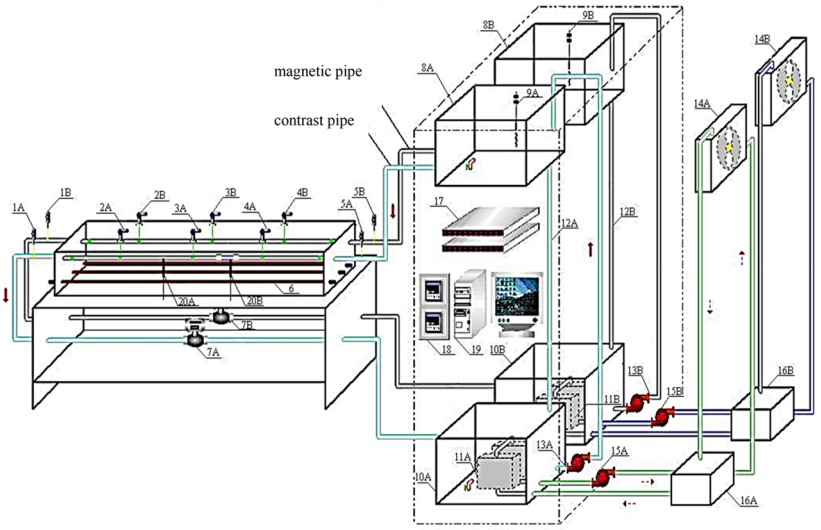

(a)

(b)

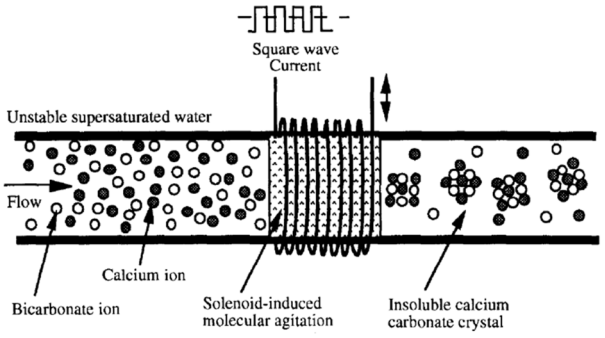

(c)

Figure 1. Water treatment technology and anti-fouling effect of the online monitoring evaluation system (research group, Jilin, China). (a) 1: Outlet temperature monitor; 2−4: water temperature monitor; 5: inlet temperature monitor; 6: electric heater; 7: flowmeter; 8: upper tank; 9: upper tank temperature monitor; 10: lower tank; 11: heat exchanger; 12: overflow pipe; 13: cooling water circulation pump; 14: air-cooled radiator; 15: air circulating pump; 16: air-cooled tank; 17: data acquisition card; 18: proportion integration differentiation (PID) controller; 19: industrial computer; 20: water bath temperature monitor. (b) Physical model of the online evaluation experiment. (c) Structure principle of the parallel electromagnetic field.

It is proved that electromagnetic water treatment has an effect on many physical and chemical properties of water.[6] It is hard to distinguish which parameter can establish a closer relationship with the electromagnetic frequency to better reflect the effect of scale removal and inhibition. The treatment effects of electromagnetic fields are mostly focused on the action of various factors that influence fouling.[7] In ref 8, to study the influence of the particle property to fouling forming, a deposition and scaling model is set up. A processing of particle fouling under conditions of different particle properties is simulated in Fluent with the method of CFD. In order to investigate the microbial fouling characteristics in a Ca^{2+} environment, having the artificial ratio method adopted to add iron bacteria and $CaCl_2$ into the heat exchanger's recirculating cooling water system was implemented so that the cooling water system's fouling characteristics at different

https://doi.org/10.1021/acsomega.1c02193
ACS Omega 2021, 6, 28515−28527

temperatures, velocities, and iron bacterial concentration can be studied.[9,10] CFD simulation is performed to study the heat and mass transfer coefficients of the alternating absorber of staggered tube bundle with M-W mesh guiders. The CFD simulation results of liquid film velocity, temperature, and concentration are obtained in the literature.[11] Reference 12 calculates and analyzes gravitational force, adhesive force, Saffman force, Magnus force, and fluid resistance under different particle diameters of Pearl River water, silt particle, and lake water blending with silt, respectively. The adhesion and abrasion effects of different forces under different flow rates qualitatively are educed. The corresponding change relation of various factors under the influence of electromagnetic parameters has rarely been studied.

The fundamental research on water quality parameters (conductivity, fouling induction period (FIP), scanning electron microscopy, and particle size distribution) in the process of circulating cooling water flowing through the heat exchange tube, which is under the impact of different magnetic induction intensities, has been carried out.[13] The parameters of solution such as conductivity, pH value, zeta potential of colloidal particles, and surface tension will change with the change of electromagnetic fields, and eventually will directly affect the formation and growth process of fouling.[14] The variable frequency electromagnetic water treatment method acts on different water bodies, and the treatment effect is also different due to different electromagnetic frequencies; therefore, there are still many problems to be studied in this field.[15,16] Magnetic field lines can indeed be perpendicular to the water flow direction. Based on the variation of water quality parameters (conductivity, pH value, dissolved oxygen, turbidity) under the influence of the frequency conversion electromagnetic field, the relationship between conductivity, pH value, and magnetic acting time was analyzed by using the correlative degree analysis, balanced adjacent degree method.[17] Then, the relationship between conductivity, pH value, dissolved oxygen, turbidity, and magnetic acting time was analyzed by using SPSS statistical methods.[18]

This paper focuses on the dynamic simulation results of the velocity field and pressure field of circulating cooling water on calcium carbonate fouling formation in industrial heat exchanger tubes with a straight shape and U-shaped ones under the action of 0.5, 0.75, 1, and 1.5 kHz electromagnetic fields by using Fluent software. Variations in the flow state of circulating cooling water reflect the formation process of fouling from different aspects. Based on an experimental platform with structure principle of a parallel electromagnetic field,[13,17] we study the velocity field and pressure field at various points in the process of circulating cooling water flowing through the heat exchange tube combined with Fluent dynamic analysis.[18,19] The experimental data of fouling resistance on the heat exchange surfaces in 0.5, 0.75, 1, and 1.5 kHz magnetic and contrast experiments are carefully analyzed by Origin. Dynamic analysis is employed to indicate the significance of the flow state of circulating cooling water in the fouling formation process.[20] The degrees and effects of heat transfer and the flow states of circulating cooling water are obtained to study the formation process of fouling and further explore the electromagnetic anti-fouling theory.

2. MATERIALS AND METHODS

2.1. Experimental System. The principle of water treatment technology and anti-fouling effect of online monitoring evaluation experiment is displayed in Figure 1. An experimental platform with magnetic and contrast treatments is proposed, and the flow states of circulating cooling water and characteristics of fouling resistance are studied with the same heat exchange condition.[13,18,21] Additionally, due to the influence of the electromagnetic field, the formation of coarse particulate fouling is inhibited.

The experimental platform focuses on calcium carbonate ion concentration, which is more conducive for drawing electromagnetic anti-fouling conclusions. Reducing the time for fouling formation from 1 or 2 years to approximately 7 days simulates the heat exchanger fouling process, allowing rapid fouling to be achieved. While setting the constant temperature water tank to 50 °C, the solution of calcium carbonate, which is with high hardness of 1000 mg/L, flows through thin stainless steel or copper pipes at 29 °C. Five groups of polyvinyl chloride (PVC) pipes wound with insulated copper wire are buckled at one circulating cooling water tube that is used in the heat exchanger. Based on the self-developed variable frequency electromagnetic water treatment equipment, a 3 A alternating current with a square signal output is produced and two ends of the insulated copper wire coil is connected, making the magnetic field lines parallel to the water flow direction. A nonmagnetic contrast experiment is conducted in the other circulating cooling water tube. Through the regulating valve of the upper tanks, the circulating cooling water flow velocity is maintained at 0.4 m/s. In order to ensure collection and reliability of experiment data, the inlet temperature of circulating cooling water and fouling resistance are measured every 3 h.

2.2. Calculation of Magnetic Field Intensity in the Experimental Pipeline. In the process of electromagnetic water treatment, magnetic field intensity is closely related to the effect of magnetic treatment. Therefore, before simulating the flow state of circulating cooling water in the experimental pipeline, the magnetic field intensity produced by the variable-frequency electromagnetic device in the inlet section is statistically calculated, allowing the formation of fouling to be more accurately simulated based on the known magnetic field intensity.

Method 1: As shown in Figure 2, the angles between the Z-axis of insulated copper wire coil and the lines of point in the

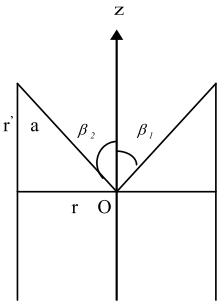

Figure 2. Electromagnetic structure of wire coil.

Z-axis and the ends of pipeline are β_1 and β_2, respectively. The radius is r, the length is L, the turns are W, and the current is I. The distance between the center point and the field point is a. The magnetic induction intensity at any point of the Z-axis is then

https://doi.org/10.1021/acsomega.1c02193
ACS Omega 2021, 6, 28515−28527

$$B = \frac{\mu IW(\cos\beta_1 + \cos\beta_2)}{2L} \quad (1)$$

where $\mu = 4\pi \times 10^{-7}$ H/m represents the air permeability.[22,23] While the point is at the center of the Z-axis, $r \ll L$, and then

$$\cos\beta_1 = \cos\beta_2 = \frac{\frac{L}{2}}{\sqrt{r^2 + \frac{L^2}{2^2}}} \approx 1 \quad (2)$$

Method 2: If the cross-sectional area of wire coil is A, the magnetoresistance can be represented as follows:

$$R = \frac{L}{\mu A} \quad (3)$$

The magnetomotive force is

$$F = WI = \Phi R \quad (4)$$

When the area S is vertical to B, then B can be calculated according to the following eq 5:

$$\Phi = BS = BWA, \quad (5)$$

During the process of actual experiments, the gauss meter is employed to directly and accurately measure the magnetic field intensity of the points in wire coil while simultaneously taking into consideration the relationship between B, rated voltage, output current, and magnetic field intensity H.[24,25] This research serves as a reference for obtaining more experimental data, analyzing the pipeline heat transfer process, and discussing the electromagnetic anti-fouling performance under the influence of electromagnetic fields.

The coupling between a fluid flow field and a magnetic field can be obtained based on two basic actions: the inducted current due to the motion of conductive materials in the magnetic field, and the Lorentz force due to the electrical effect, which leads to the interaction between the current and the magnetic field. However, inducted currents and Lorentz forces are usually the opposite of the mechanism by which they are produced. Thus, the resulting Lorentz force will systematically cause an electromagnetic-induced motion. The electromagnetic induction phenomenon also occurs in the process of alternating magnetic fields.

Maxwell's equations describe the electromagnetic field:

$$\nabla \times \underset{B}{\rightarrow} = 0, \quad (6)$$

$$\nabla \times \vec{E} = -\frac{\partial \vec{B}}{\partial t}, \quad (7)$$

$$\nabla \cdot \vec{D} = q, \quad (8)$$

$$\nabla \times \vec{H} = \vec{j} + -\frac{\partial \vec{j}}{\partial t}, \quad (9)$$

Here, $\underset{B}{\rightarrow}$ (T) and $\underset{E}{\rightarrow}$ (V/m) are the magnetic induction intensity and electric field intensity, and $\underset{H}{\rightarrow}$ (A/m) and $\underset{D}{\rightarrow}$ (C/m^2) are the magnetic field intensity and electric field flux density, respectively. q (C/m^3) is the charge density, and $\underset{j}{\rightarrow}$ (A/m^2) is the current density. In the magnetic field, $\underset{H}{\rightarrow}$ and $\underset{D}{\rightarrow}$ is defined as follows:

$$\underset{H}{\rightarrow} = \frac{1}{\mu} \underset{B}{\rightarrow}, \quad (10)$$

$$\underset{D}{\rightarrow} = \varepsilon \underset{E}{\rightarrow}, \quad (11)$$

The μ (H/m) and ε (F/m) here are the magnetic permeability and dielectric constant, respectively. It is important to obtain the current density when studying the interaction between the fluid flow field and the magnetic field. The current density can be estimated by solving the magnetic induction equation and the potential equation.

2.3. Dynamic Analysis. In this paper, we employ Fluent for numerical simulation. Fluent is a computational fluid dynamics CFD software package, which is widely applied in industrial production, especially in heat transfer, fluids, etc. In Fluent, all of the flows can be modeled and calculated through solving the mass and momentum conservation equations. Fluent mainly solves viscous incompressible flow in which density is constant. The conditions of heat transfer can be modeled and calculated by solving the mass and momentum conservation equations. The compressibility of water is small, signifying that for each additional atmospheric pressure, the volume of water only changes by one in ten thousand, making water exhibit incompressible flow. In the turbulent state of multiphase flow, the velocity field and pressure field will appear. Considering that actual data cannot always be described by a theoretical distribution, the inherent characteristics of viscous incompressible flow and relationships among variables were studied using Fluent software (Fluent 14.0, ANSYS 17.0, Inc., Canonsburg, PA, USA, 2017) combined with Origin software (Origin Pro8.0, OriginLab, Hampton, Massachusetts, United States, 2008). These programs can vividly and effectively solve the issue of fluid calculation through their simulation process.

There are two key sections in the Fluent numerical simulation process: pre-module ICEM CFD and the Fluent solver. Tecplot is a data visualization program that can realize post-processing function.[26] The flow state of circulating cooling water can be pre-processed by ICEM CFD and calculated by Fluent solver. Tecplot is finally applied for further processing and obtaining the effect graph of fouling formation process.[27]

Pipeline flow is very common in real life and industrial production process, such as the fluid flow in a heat exchanger. Also, Fluent has provided a more comprehensive simulation environment and process. The experimental conditions will be detailedly simulated and analyzed in this paper. ICEM CFD (draw the calculation area and the type of relevant specified boundary condition) exports mesh file, then imports Fluent solver (settings), forms the case file and solves the situation, and finally imports Tecplot visual processing software for further simulation.

2.4. Evaluation Metrics. Due to the increased fouling, fouling resistance is known as a coefficient of measurement for the heat exchange surface. Variation in fouling resistance is closely related to the magnetic field intensity and heat exchange equipment working conditions.[28] Anti-fouling efficiency, which is a measurement of fouling inhibition effects, can be calculated as follows:

$$\eta = \frac{R_{f0i} - R_{f1i}}{R_{f0i}}, \quad (12)$$

https://doi.org/10.1021/acsomega.1c02193
ACS Omega 2021, 6, 28515−28527

where R_{f0i} denotes the fouling resistance value in the contrast experiment at moment i, and R_{f1i} denotes the fouling resistance value in the magnetic experiment at moment i. The average anti-fouling efficiency can be expressed as

$$\bar{\eta} = \sum_{i=1}^{n} \eta_i, \tag{13}$$

where n denotes the experimental data number.[29,30]

2.5. Epsilon Turbulence Model. Since the 1960s, researchers have proposed different schemes for the selection of a characteristic parameter Z, which characterizes the turbulence effect. Thus, various bilateral models are established. The k-ε model is the most mature and widely used, where ε is the dissipation rate of turbulent energy. A generalized transport equation of turbulence parameter Z can be established as

$$Z = k^m l^n, \tag{14}$$

where m and n are constants. The k equation after simulation is

$$\frac{\partial}{\partial t}(\rho k) + \frac{\partial}{\partial x_j}(\rho U_j k) = \frac{\partial}{\partial x_j}\left(\frac{u_{eff}}{\delta_k}\frac{\partial k}{\partial x_j}\right) + G - C_D \rho k^{3/2} \tag{15}$$

The ε equation after simulation is:

$$\begin{aligned} &\frac{\partial}{\partial t}(\rho \epsilon) + \frac{\partial}{\partial x_j}(\rho U_j \varepsilon) \\ &= \frac{\partial}{\partial x_j}(\rho U_j \varepsilon) \\ &= \frac{\partial}{\partial x_j}\left(\frac{u_{eff}}{\sigma_\epsilon}\frac{\partial \varepsilon}{\partial x_j}\right) + \frac{\varepsilon}{k}(C_1 G - C_2 \rho \varepsilon) \end{aligned} \tag{16}$$

The calculation of the k differential transport equation is the same as that of the single equation model, which is simulated term by term from the precise transport equation and has certain theoretical and experimental basis.

The k-epsilon turbulence model is the most common turbulence model. It is widely employed in the industrial flow simulation due to its good robustness, economy, and reasonable prediction of the turbulence effect. The k-epsilon turbulence model is a two-equation model, which is suitable for fully developed turbulence, but the calculation results are not ideal for the practical engineering application of transition conditions and near-wall regions with a low Reynolds number (laminar flow). Based on the water treatment technology and anti-corrosion effect of online monitoring evaluation experimental and simulation conditions in this paper, the high Reynolds number is carried out on the assumption that the flow of the circulating cooling water is completely turbulent, and the influence of molecular viscosity is negligible.[31]

Equations 15 and 16 are combined as the standard two-equation k-ε turbulence model. Using ε instead of characteristic length l, the expression of turbulence viscosity coefficient in the k-ε model is obtained:

$$\mu_t = C_\mu \rho k^2/\varepsilon, \tag{17}$$

The standard k-ε model is a semi-empirical formula with a wide range of applications, economical application, and reasonable accuracy. The turbulent kinetic energy transport equation is derived by a precise equation, and the dissipation rate equation is obtained by physical reasoning and mathematical simulation of a similar prototype equation.

This paper studies mainly the flow states of circulating cooling water in heat exchange tubes under the action of electromagnetic fields. The circulating working medium is an incompressible fluid, so that the inlet boundary conditions change along with the change of working conditions, and the free outflow of fluid is the export boundary condition. Other boundary conditions are set as wall insulation, fluid without sliding and zero pressure gradient. Without considering the gravity factor, the standard wall function is selected for near-wall treatment.

3. RESULTS AND DISCUSSION

Pipeline flow is very common in real life and industrial production processes, such as the fluid flow in a heat exchanger. Through using the ICEM pre-treatment and modeling by the Fluent solver, we can learn the commands about copy, move, split, unite, and surface mesh, volume mesh division, etc. Also, in the post-visual process of Tecplot, it can be clearly observed that the pipeline fluid flow at the initial speed of 0.4 m/s by using animation display of pathlines (streamline). The experimental conditions are carefully analyzed and proposed in the second section. As an incompressible viscous fluid, the circulating cooling water flows from the inlet to the outlet at a speed of 0.4 m/s and its velocity and pressure are different at points of different pipelines.

Figure 3 shows the working condition of heat exchange tube of water treatment technology and anti-corrosion effect of online monitoring evaluation experiment, where the radius is r = 2.2 cm, the thickness is h = 0.2 cm, and the length is L = 220 cm.

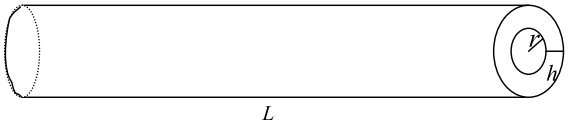

Figure 3. Structure of the circular pipeline (research group, Jilin, China).

Figure 4 shows the working condition of heat exchange tube of the improved experiment, where the radius of the straight pipeline is r = 2.2 cm, the thickness of the pipeline is h = 0.2 cm, the length of the straight pipeline is L = 220 cm, and the radius of the U-shaped pipeline is R = 20 cm.

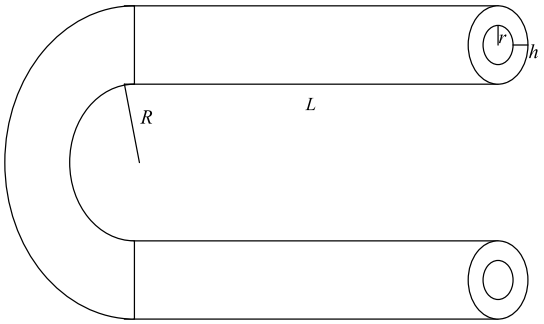

Figure 4. Structure of the U-shaped pipeline (research group, Jilin, China).

https://doi.org/10.1021/acsomega.1c02193
ACS Omega 2021, 6, 28515−28527

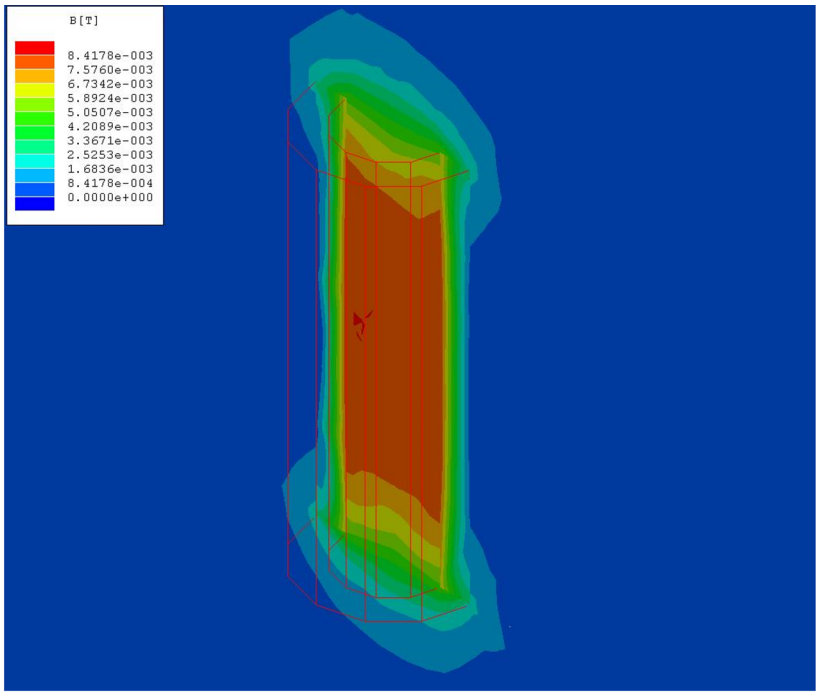

(a)

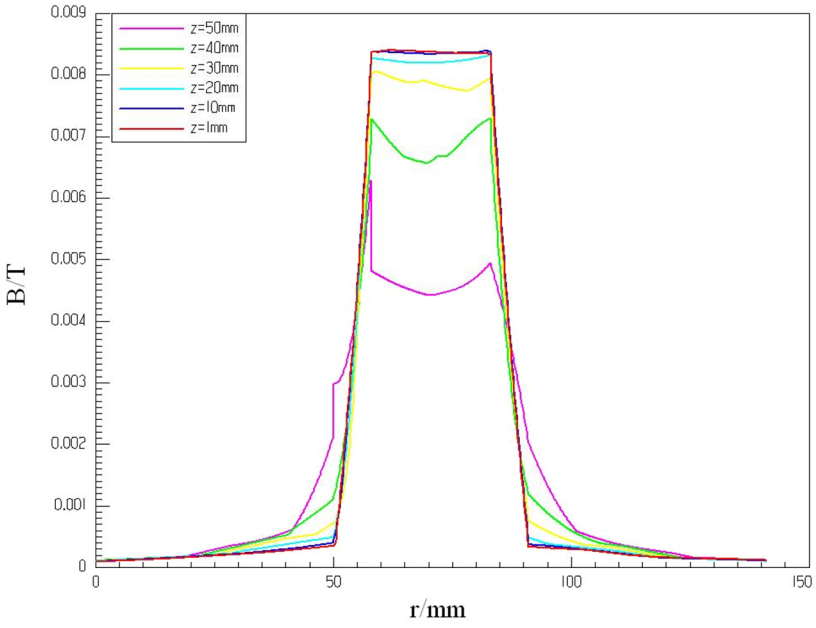

(b)

Figure 5. (a) Steady-state magnetic induction intensity of electrified solenoid. (b) Magnetic induction intensity of different locations from the center of the *Z*-axis.

3.1. Three-Dimensional Fluid Flow State of the Circular Pipeline. The simulation results of steady-state magnetic induction intensity of an electrified solenoid are shown in Figure 5a. The magnetic induction intensity inside the electrified solenoid is greater than that outside the solenoid. The magnetic induction intensity at the internal center is the largest, which can reach 84 Gs. The magnetic induction intensity decreases with the increase of the distance from the center to ends, and the damping speed of the magnetic induction intensity is faster with the increasing distance from the center of the solenoid.[32] Therefore, the magnetic induction intensity at both ends of the solenoid is much smaller than that at the center, which can reach several *G*s.

In order to verify the radial variation of magnetic induction intensity B when z is constant, as shown in Figure 5b, z represents the axial distance between the spatial point and the solenoid center, where the solenoid center is located at 70.5

https://doi.org/10.1021/acsomega.1c02193
ACS Omega 2021, 6, 28515−28527

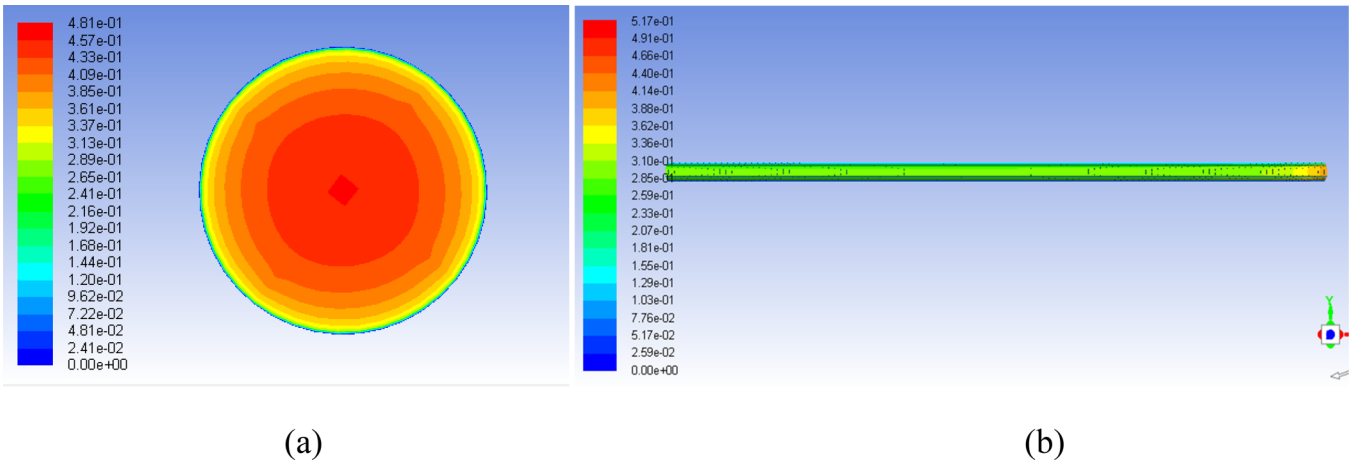

Figure 6. Velocity field in the circular pipeline (m/s). (a) Velocity field at the outlet of circular pipeline in the simulation process. (b) Velocity field on the Z-axis in the simulation process.

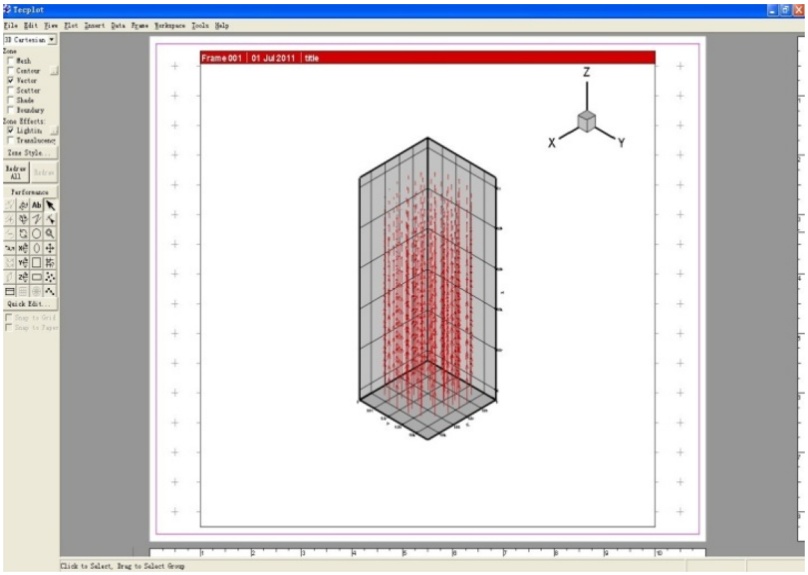

Figure 7. Certesian diagram of velocity field in Tecplot.

mm. When z is small, B increases with the increase of the radius r. In the radial direction from the solenoid, the value of B is a constant at 20−25 mm from the coil with only a small fluctuation. B then decreases with the increase of radial distance. When z is large, the increase of B is small. B also increases with the increase of r and gradually decreases. The difference is that it exhibits a damping trend while B increases to 20−30 mm from the center of the coil. B is smallest at the center of coil, signifying that around the edge of the solenoid, the magnetic induction intensity at the edge of coil is greater than that at the center. Therefore, the magnetic induction intensity at arbitrary points inside the solenoid can be determined after choosing the geometrical size of solenoid and the current parameters. Furthermore, the electromagnetic anti-fouling process can be studied from the angle of magnetic induction intensity.[33]

The velocity field of circulating cooling water in the straight pipeline is conducted, where the radius is 2.2 cm, the thickness is 0.2 cm, and the length is 220 cm. The ICEM pre-treatment of Fluent is used to draw grids. The number of grids must satisfy the requirement of non-overlapping grids at different locations, and it is very important for the simulation. Here, the number of grids is set to 220. The non-overlapping grid distribution is provided on the surface of the entrance and exit areas. It can be seen that the grids are non-overlapping and evenly distributed. Figure 6a shows the velocity field at the outlet of pipeline with inlet velocity of 0.4 m/s. The right side of Figure 6b shows the inlet of pipeline. The speed value in the red area is larger than others. It can be noticeably observed that the velocity of the circulating cooling water is larger when it leaves the outlet of the pipeline and the other areas are slightly smaller. There is the velocity stratification at the outlet of pipeline, and the closer to the center of the heat exchange tube, the greater the velocity of circulating cooling water is. Figure 7 shows the velocity field in the pipeline from the point of the Cartesian coordinate system. The red lines are clear and smooth, and the circulating cooling water flows evenly in the straight circular pipeline.

The circulating cooling water near the edge of heat exchange tubes is affected by the friction caused by the hydraulic pressure and loses a part of the kinetic energy. Therefore, the slow velocity of the circulating cooling water at the outlet of

https://doi.org/10.1021/acsomega.1c02193
ACS Omega 2021, 6, 28515−28527

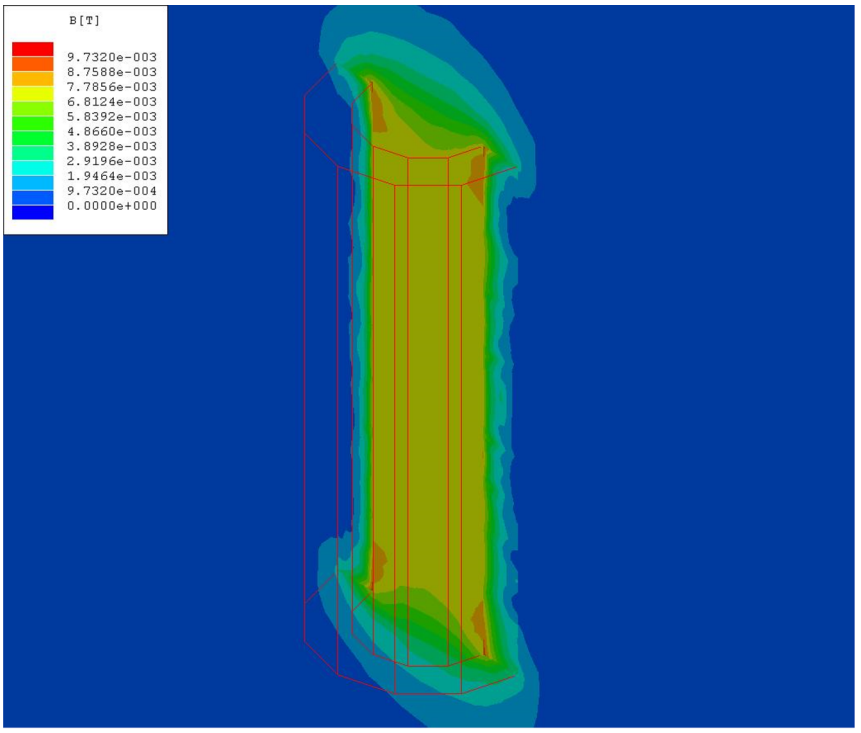

(a)

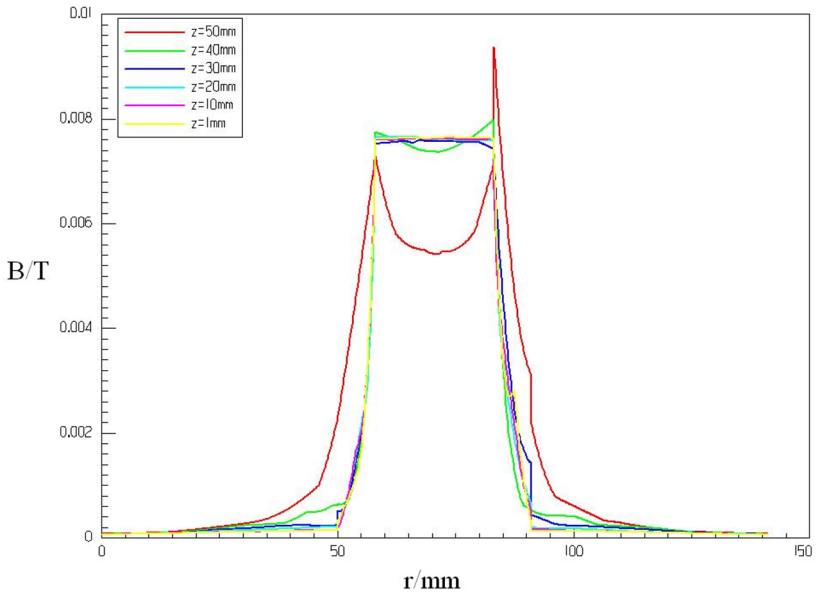

(b)

Figure 8. (a) Alternating magnetic induction intensity of the electrified solenoid. (b) Magnetic induction intensity of different locations from the center of the *Z*-axis.

pipeline will further promote the formation process and adhesion of fouling on the surface of heat exchange tubes. Near the circulating pipe wall, the working medium flow speed is slow and the scouring effect on the heat exchange tube is small, so there will be scale on the heat exchange tube wall.

3.2. Three-Dimensional Fluid Flow State of the U-Shaped Pipeline. The simulation results of alternating magnetic induction intensity of the electrified solenoid are shown in Figure 8a, demonstrating that the internal magnetic induction intensity of the electrified solenoid is much greater than the external magnetic induction intensity and that distribution of internal magnetic induction intensity is uniform. The average magnetic induction intensity of the interior solenoid can reach up to 77 Gs, which is much larger than that of the steady magnetic field, demonstrating that when the square wave current is applied alternately in the coil, the

https://doi.org/10.1021/acsomega.1c02193
ACS Omega 2021, 6, 28515−28527

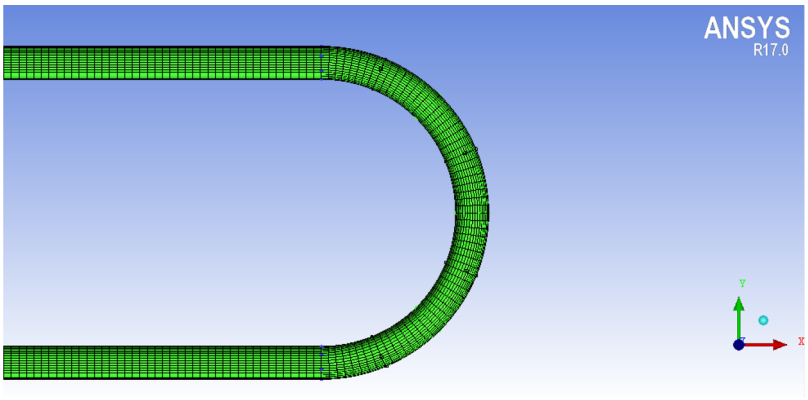

Figure 9. U-shaped pipeline grid diagram.

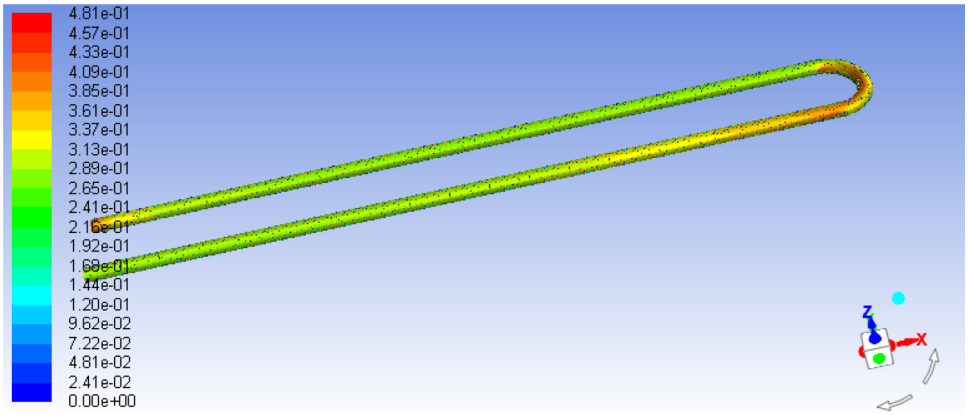

Figure 10. Velocity field of the U-shaped pipeline (m/s).

alternating magnetic field will be produced, and the alternating magnetic field with time will excite the induced electric field. Then, the alternating change of the induced electric field with time will again excite the additional magnetic field, which will be excited in turn. Therefore, the total magnetic field inside the electrified solenoid can be classified as the superposition of the magnetic field generated by current and a series of additional magnetic fields. This determines that the magnetic induction intensity is relatively high.

In order to verify the radial variation of magnetic induction intensity B when z is constant, as shown in Figure 8b, z represents the axial distance between the spatial point and the solenoid center, and the solenoid center is located at 70.5 mm. When z is constant, B increases with the increase of r. In the radial direction from solenoid, the magnetic induction intensity tends to be stable when the radial distance from the Z-axis is 15−20 mm, and then it decreases with the increase of the r value. From the simulation results, the magnetic induction intensity of each point of the axial distance is not very different and more uniform when z is below 40 mm. Furthermore, the magnetic induction intensity of the point at the axial edge fluctuates greatly when z is between 40 and 50 mm.

The velocity field and pressure field of circulating cooling water are conducted in this section, where the radius and length of the straight pipeline part are 2.2 and 220 cm, respectively, and the radius of the U-shaped part is 20 cm. It is very important for the simulation to have the number of grids in Figure 9 satisfy the requirement of non-overlapping grids at different locations, especially for the U-shaped part. Here, the number of grids is set to 220, and the number of grids is set to 68 at the bend. Non-overlapping grids are provided on the surface of the entrance and exit areas of the pipeline. It can be seen that the grid distribution at the bend is non-overlapping and evenly distributed. The iteration will terminate when the accuracy requirement is satisfied, and in this simulation, the requirement can be satisfied after 100 iterations. The circulating cooling water fills the entire heat exchanger tube, and the heat transfer process is sufficient, which demonstrates one of the satisfactory conditions of fouling formation. In Figure 10, the red area indicates that the velocity value is slightly larger than others, which means that the change of circulating cooling water flow state with the pipeline shape will cause a certain impact to fluid velocity. In Figure 11, the red area represents the outlet of the pipeline, so the pressure value at the outlet is larger. The pressure value of the inside part of the U-shaped pipeline is noticeably smaller. In other words, the impact on the inner side of the pipeline is small when the circulating cooling water flow state changes following the change of pipeline shape. Fouling runs are carried out in pipelines with different shapes and heat transfer surfaces by the entire simulation process.

In the U-shaped pipeline, it can be obtained that the flow velocity of the circulating cooling water is uniform in the straight part of the heat exchange tube. Then, the flow direction of circulating cooling water is changed in the U-shaped part due to the turbulence effect. The velocity at the outlet of the heat exchange tube is large. The pressure outside the U-shaped part is greater than the pressure inside the U-shaped part. The velocity and pressure of circulating cooling water in the heat exchange tube have great impact on the

https://doi.org/10.1021/acsomega.1c02193
ACS Omega 2021, 6, 28515−28527

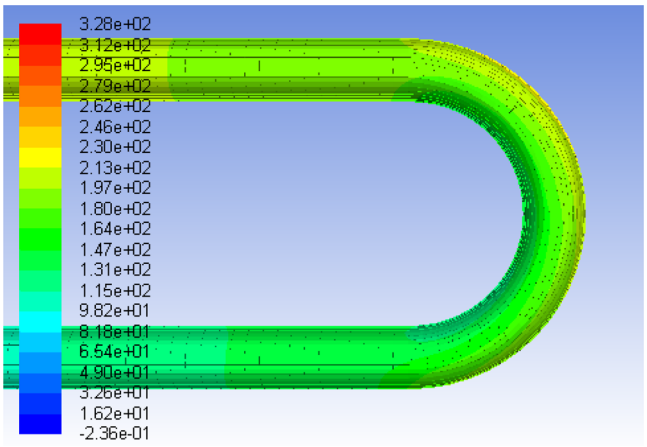

Figure 11. Pressure field of the U-shaped pipeline (kg/m·s^2).

fouling on the tube wall, which means that the fouling is not easy to be produced, the fouling resistance value will be small, but the heat exchange tube is easy to be eroded. The numerical simulation process can also reflect the state of fouling attached to the tube wall.

3.3. Fouling Inhibition Performance Analysis. Dichotomy is employed to investigate the influence of electromagnetic frequencies on fouling resistance. Figure 12 displays the inhibitory effects of electromagnetic fields on fouling in 0.5, 0.75, 1, and 1.5 kHz magnetic experiments. Results show that variations in fouling resistance in magnetic experiments tend to be different from those in contrast experiments. After the end of the induction period, the fouling resistance on the surface of the two heat exchange tubes begins to rise, and eventually, it stabilizes to some value. The induction period refers to the period from the moment when the solution reaches supersaturation to the arrival of crystallized sediment. Fouling resistance on the surface of the magnetic heat exchange tube is smaller than that of the nonmagnetic one when the initial values return to zero. The result indicates that the induction period of fouling on the surface of the heat exchange tube under the action of electromagnetic fields can be relatively prolonged. After calculating eqs 6 and 7, the value of antifouling efficiency in 0.5, 0.75, 1, and 1.5 kHz magnetic and

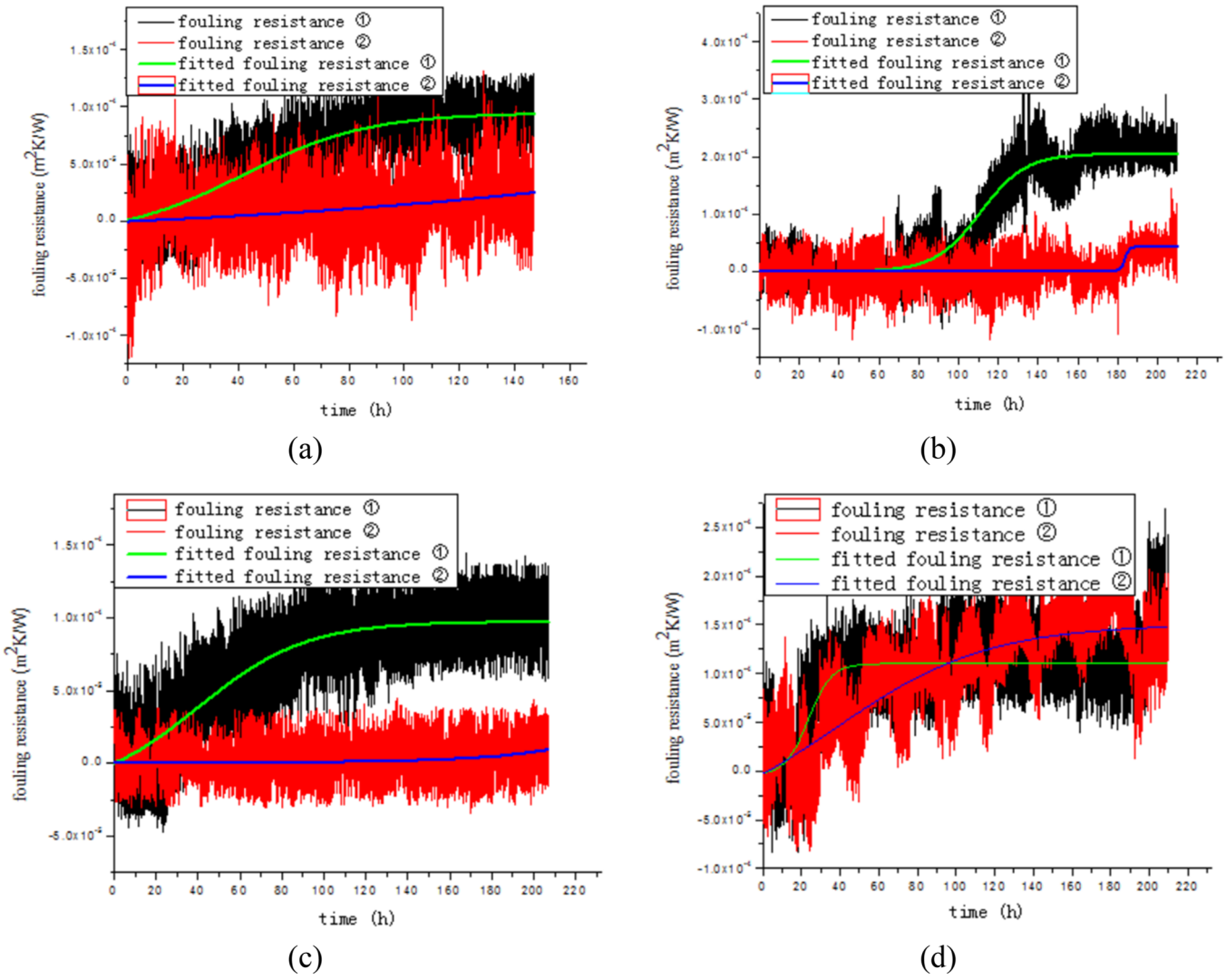

Figure 12. Trend diagram of fouling resistance in the experimental process. (a) Fouling resistance in 0.5 kHz magnetic and contrast experiments. (b) Fouling resistance in 0.75 kHz magnetic and contrast experiments. (c) Fouling resistance in 1 kHz magnetic and contrast experiments. (d) Fouling resistance in 1.5 kHz magnetic and contrast experiments. ① Contrast experiment data. ② Magnetic experiment data.

https://doi.org/10.1021/acsomega.1c02193
ACS Omega 2021, 6, 28515−28527

contrast experiments are 46.8, 84.8, 91.2, and 63.6%, respectively. The growth rate of fouling resistance in magnetic experiments is also smaller than that in contrast experiments. Better anti-fouling performances are obtained under the action of about 1 kHz electromagnetic frequency.

In this paper, the Fluent software is used to simulate the pressure field and velocity field distribution of circulating cooling water in heat exchange tubes under the action of electromagnetic fields to explore the fouling generation mechanism. Figure 13 is added to show separately the results

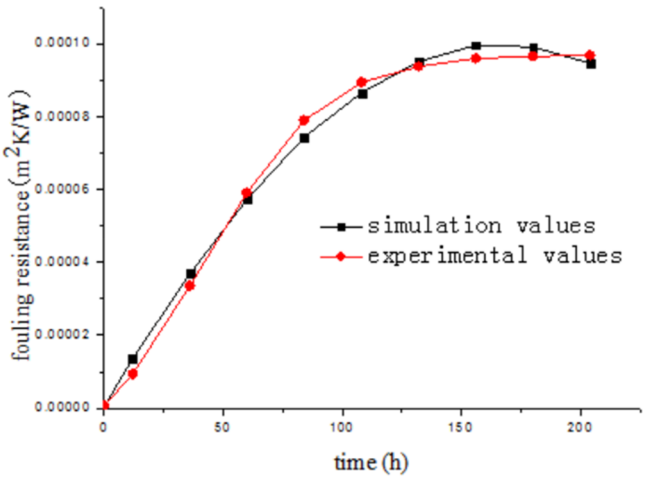

Figure 13. Comparison diagram of simulation values and experimental values of fouling resistance.

of fouling resistance based on the Fluent numerical simulation and the water treatment technology and anti-fouling effect of online monitoring evaluation experiment under non-magnetic conditions, so as to verify the effectiveness of the pressure field and velocity field of circulating cooling water obtained by the standard k-ε model of Fluent software.

In order to evaluate quantitatively the accuracy of the standard k-ε model, the absolute percentage error can be expressed as:

$$e_{\mathrm{MAMPE}} = 100 \times \frac{\sum_{i=1}^{n} |(R_{fi} - \widehat{R_{fi}})/R_{fi}|}{n},\ n = 10 \qquad (18)$$

where R_{fi} and $\widehat{R_{fi}}$ denote the experimental value and the simulation value of the fouling resistance at moment i, respectively. The absolute percentage error is 5.0315 by calculation, so it meets the needs of the engineering veracity. The results show that it is feasible for the numerical simulation study on the formation process and adhesion of fouling on the surface of heat exchange tubes by using Fluent software.

As shown in Figure 14, the velocity field and pressure field are simulated under the influence of electromagnetic frequencies. It is clear that magnetic parameters have influence on fouling inhibition and flow states of circulating cooling water. The flow velocity in the area with high surface pressure of circulating cooling water is relatively small, which is the result of more energy loss caused by a larger friction force. In the area with large flow velocity, the washing effect of circulating cooling water on the heat exchange tube is also large, and the fouling will be washed to a certain extent, so the fouling in this area is less. However, the corrosion appearing on

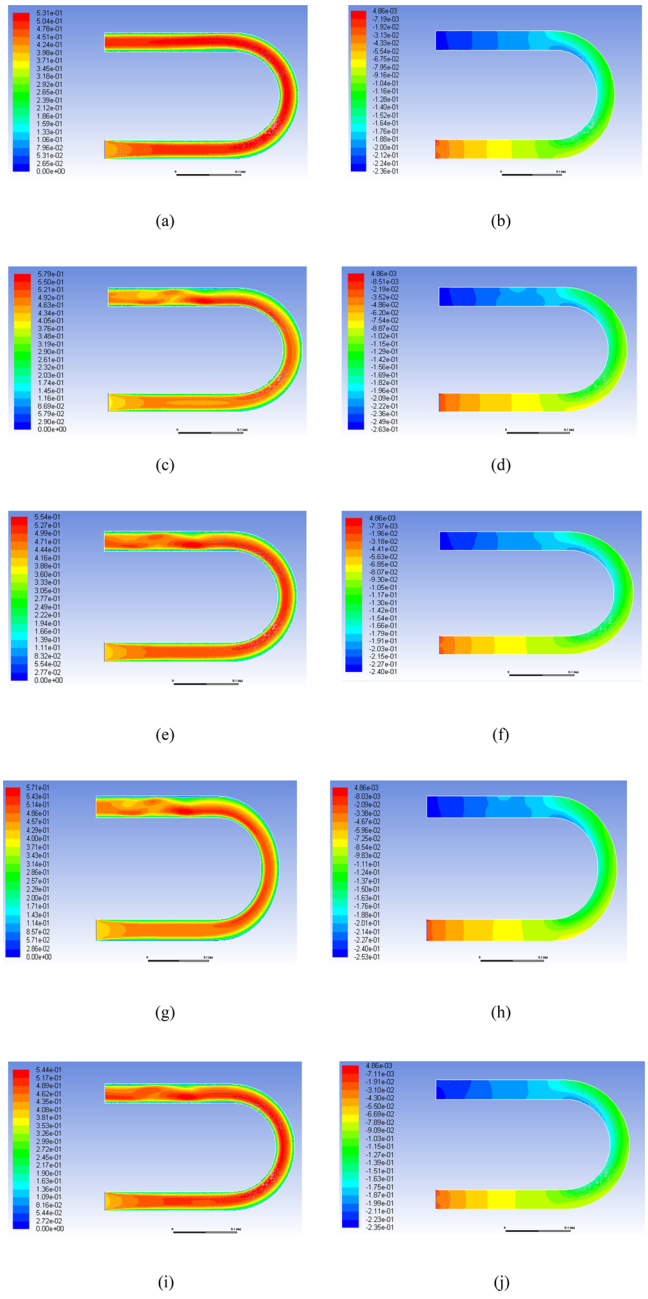

Figure 14. Trend diagram of the velocity field (m/s) and pressure field (kg/m·s^2) on the Z-axis in the simulation process. (a) Velocity field under a non-magnetic condition. (b) Pressure field under a non-magnetic condition. (c) Velocity field under a 0.5 kHz magnetic condition. (d) Pressure field under a 0.5 kHz magnetic condition. (e) Velocity field under a 0.75 kHz magnetic condition s. (f) Pressure field under a 0.75 kHz magnetic condition. (g) Velocity field under a 1 kHz magnetic condition. (h) Pressure field under a 1 kHz magnetic condition. (i) Velocity field under a 1.5 kHz magnetic condition. (j) Pressure field under a 1.5 kHz magnetic condition.

the area with a large scour effect is more likely to be caused, which makes the heat exchange tube damaged.

Electromagnetic water treatment technology can have great influence on the formation process of fouling. Variations in fouling resistance provide application guidance on the practical application of electromagnetic field anti-fouling, fouling removal, and corrosion inhibition performance. Velocity field and pressure field can be employed as important contents in

https://doi.org/10.1021/acsomega.1c02193
ACS Omega 2021, 6, 28515−28527

the study of fluid dynamic field for the heat exchange process. Moreover, the flow states of circulating cooling water can be further studied to reflect the electromagnetic anti-fouling mechanisms.

4. CONCLUSIONS

In this study, the dynamic simulation results of the velocity field and pressure field of circulating cooling water were conducted on calcium carbonate fouling formation in industrial heat exchanger tubes with a straight shape and U-shaped ones, respectively, by using Fluent software. Based on a self-designed online evaluation experimental platform of the electromagnetic anti-fouling effect, the experimental data of fouling resistance on the heat exchange surfaces by employing Origin is obtained.

The flow state of the circulating cooling water is uniform in the straight pipeline, and the velocity of the circulating cooling water is smaller in the outlet of the pipeline. The pressure on the surface of circulating cooling water is inversely proportional to the velocity when the heat exchanger tube changes from the straight tube to the U-shaped tube. The velocity and pressure of circulating cooling water in the heat exchange tube have great impact on the fouling on the tube wall, and the fouling is not easy to be produced. The numerical simulation process can reflect the state of fouling attached to the tube wall. The experimental results indicate that fouling resistance on the surface of the magnetic heat exchange tube is smaller than that of the nonmagnetic one when the initial values return to zero. The pace for fouling formation is slowed down. The anti-fouling efficiency in 0.5, 0.75, 1, and 1.5 kHz magnetic and contrast experiments are 46.8, 84.8, 91.2, and 63.6%, respectively. Better anti-fouling performances are obtained under the action of about 1 kHz electromagnetic frequency.

AUTHOR INFORMATION

Corresponding Author

Fang He − *School of Technology, Beijing Forestry University, Beijing 100083, China;* orcid.org/0000-0003-2518-4822; Phone: +86-1371-889-2180; Email: hf1986@bjfu.edu.cn

Authors

Lei Yan − *School of Technology, Beijing Forestry University, Beijing 100083, China*

Xiao Qi − *Energy and Electricity Research Center, Jinan University, Zhuhai 519070, China*

Xing Han − *Chip Development Center, Beijing Zhixin Microelectronics Technology Co., Ltd, Beijing 102200, China*

Jianguo Wang − *School of Automation Engineering, Northeast Electric Power University, Jilin 132012, China*

Complete contact information is available at: https://pubs.acs.org/10.1021/acsomega.1c02193

Author Contributions

Methodology was done by F.H. Formal analysis was done by X.Q. Technical guidance was provided by X.H. Data curation was done by J.G.W.; The project was administered by L.Y. Writing of the original draft was prepared by F.H. Writing of the review and editing was done by X.Q.

Funding

This research received no external funding.

Notes

The authors declare no competing financial interest.

ACKNOWLEDGMENTS

This research was supported by the Fundamental Research Funds for the Central Universities (grant no. BLX201604), the National Natural Science Foundation of China (grant no. 51176028), and the Natural Science Foundation of Jilin Province, China (grant no. 201115179).

REFERENCES

(1) Steinhagen, R.; Müller-Steinhagen, H.; Maani, K. Problems and costs due to heat exchanger fouling in new zealand industries. *Heat Transfer Eng.* **1993**, *14*, 19−30.

(2) Roussak, O. V.; Gesser, H. D. *Applied chemistry: Textbook for engineers and technologists*; 2nd ed.; Springer: Berlin, Germany, 2013; pp 240−269.

(3) Tijing, L. D.; Kim, H. Y.; Lee, D. H.; Kim, C. S.; Cho, Y. I. Physical water treatment using RF electric fields for the mitigation of $CaCO_3$ fouling in cooling water. *Int. J. Heat Mass Transfer* **2010**, *53*, 1426−1437.

(4) Kim, W. T.; Cho, Y. I.; Bai, C. Effect of electronic anti-fouling treatment on fouling mitigation with circulating cooling-tower water. *Int. Commun. Heat Mass Transfer* **2001**, *28*, 671−680.

(5) Cravero, C.; De Domenico, D.; Ottonello, A. Uncertainty Quantification Approach on Numerical Simulation for Supersonic Jets Performance. *Algorithms* **2020**, *13*, 130.

(6) Babakhani, D. Analytical approach based on a mathematical model of an air dehumidification process. *Braz. J. Chem. Eng.* **2013**, *30*, 793−799.

(7) Chung, J.; Kang, H.; Kim, J.-O. Changes in the properties of a solution using pulsed electric field treatment as pretreatment of membrane filtration. *Desalin. Water Treat.* **2016**, *57*, 26758−26764.

(8) Li, N.; Zhang, N.; Yang, Q.; Zhong, H. W.; Yan, L. Numerical simulation of particle fouling on the heat exchange surface under different particle properties. *J. Qingdao Univ.* **2018**, *33*, 97−101.

(9) Xu, Z. M.; Jia, Y. Y.; Wang, B. L.; Zhang, Y. L.; Liu, Z. D.; Wang, J. T. Experimental analysis on bio-fouling of iron bacteria on plate heat exchanger. *J. Chem. Ind. Eng.* **2014**, *65*, 3178−3183.

(10) Xu, Z. M.; Chen, Y.; Liu, Z. D.; Zhang, Y. L.; Wang, J. T. Microbial fouling characteristics of plate heat exchangers in Ca^{2+} environment. *Chem. Mach.* **2014**, *42*, 615−619.

(11) Cao, R. B. Study on alternate heat and mass transfer absorption performances of staggered tube bundle with M-W corrugated mesh guiders. Doctor's Thesis, Southeast University: Nanjing, China, 2015.

(12) Wei, R. J. Experimental study on strengthening the fouling resistance of cooling water on the inner surface of heat transfer. Master's Thesis, South China University of Technology, Guangzhou, China, 2005.

(13) Wang, J.; Liang, Y. Anti-fouling effect of axial alternating electromagnetic field on calcium carbonate fouling in U-shaped circulating cooling water heat exchange tube. *Int. J. Heat Mass Transfer* **2017**, *115*, 774−781.

(14) Parsons, S. A.; Wang, B. L.; Judd, S. J.; Stephenson, T. Magnetic treatment of calcium carbonate scale-effect of pH control. *Water Res.* **1997**, *31*, 339−342.

(15) Al-Qahtani, H. Effect of magnetic treatment on gulf seawater. *Desalination* **1996**, *107*, 75−81.

(16) Okazaki, T.; Umeki, S.; Orii, T.; Ikeya, R.; Sakaguchi, A.; Yamamoto, T.; Watanabe, T.; Ueda, A.; Kuramitz, H. Investigation of the effects of electromagnetic field treatment of hot spring water for scale inhibition using a fibre optic sensor. *Sci. Rep.* **2019**, *9*, 10719.

(17) Wang, J. G.; He, F.; Di, H. Correlation analysis of magnetic field and conductivity, pH value in electromagnetic restraint of scale formation. *CIESC J.* **2012**, *63*, 1468−1473.

(18) He, F.; Wang, J. Statistical Analysis of Circulating Water Quality Parameters under Variable-Frequency Vertical Electromagnetic Fields. *Processes* **2018**, *6*, 182.

(19) Wang, R.; Zhang, K.; Wang, G. *Fluent technology basis and application examples*; 2 nd ed.; Tsinghua University Press: Beijing, 2010; pp. 79−90.

(20) Hong, Y.; Deng, X.; Zhang, L. 3D Numerical Study on Compound Heat Transfer Enhancement of Converging-diverging Tubes Equipped with Twin Twisted Tapes. *Chin. J. Chem. Eng.* **2012**, *20*, 589−601.
(21) Polanczyk, A.; Piechota-Polanczyk, A.; Domenig, C.; Nanobachvili, J.; Huk, I.; Neumayer, C. Computational fluid dynamic accuracy in mimicking changes in blood hemodynamics in patients with acute type IIIb aortic dissection treated with TEVAR. *Appl. Sci.* **2018**, *8*, 1309.
(22) Moussa, D. T.; El-Naas, M. H.; Nasser, M.; Al-Marri, M. J. A comprehensive review of electrocoagulation for water treatment: Potentials and challenges. *J. Environ. Manage.* **2017**, *186*, 24−41.
(23) Wang, J.; Zhang, X.; Feng, Y. Experimental study of high frequency electromagnetic field on the mitigation of fouling effect. *Control Instrum. Chem. Ind.* **2010**, *37*, 83−85.
(24) Sheikholeslami, M.; Ganji, D. D. Numerical investigation of nanofluid transportation in a curved cavity in existence of magnetic source. *Chem. Phys. Lett.* **2017**, *667*, 307−316.
(25) Pankrac, V.; Kracek, J. Simple algorithms for the calculation of the intensity of the magnetic field of current loops and thin-wall air coils of a general shape using magnetic dipoles. *IEEE Trans. Magn.* **2012**, *48*, 4767−4778.
(26) Li, T.; Feng, Z.; Song, W.; Gao, R. Effect of electromagnetic water treatment on water environment and metal equipment. *Sci. Technol. Rev.* **2012**, *30*, 46−48.
(27) Han, Z.; Wang, J.; Lan, X. *Example and application of Fluent fluid engineering simulation calculation*; 1st ed.; Beijing Institute of Technology Press: Beijing, China, 2008; pp 228−249.
(28) Wang, J.; Di, H.; He, F. Electromagnetic Frequency Influence on Fouling Resistance and Electrical Conductivity. *Control Instrum. Chem. Ind.* **2012**, 761−764.
(29) Rung, H. L. A study of physical water treatment technology to mitigate the mineral fouling in a heat exchanger. Doctor's Thesis, Drexel University, Philadelphia , 2012.
(30) Tian, L.; Huang, Y.; Sun, W.; Wang, G. *Discussions on some issues of electromagnetic anti-Fouling in circulating water treatment process*; Thermal Power Branch of Chinese Society of Electrical Engineering, Jilin, China, 2010.
(31) Du, Y. G. Experimental study on fouling resistance in the inner surface of copper tubes. Doctor's Thesis, South China University of Technology, Guangzhou, China, 2004.
(32) Zhao, X. Experimental study of electromagnetic frequency on fouling suppression mechanism and effect evaluating. Master's Thesis, Northeast Electric Power University, Jilin, China, 2010.
(33) Rodriguez, C.; Smith, R. Optimization of operating conditions for mitigating fouling in heat exchanger networks. *Chem. Eng. Res. Des.* **2007**, *85*, 839−851.

https://doi.org/10.1021/acsomega.1c02193
ACS Omega 2021, 6, 28515−28527